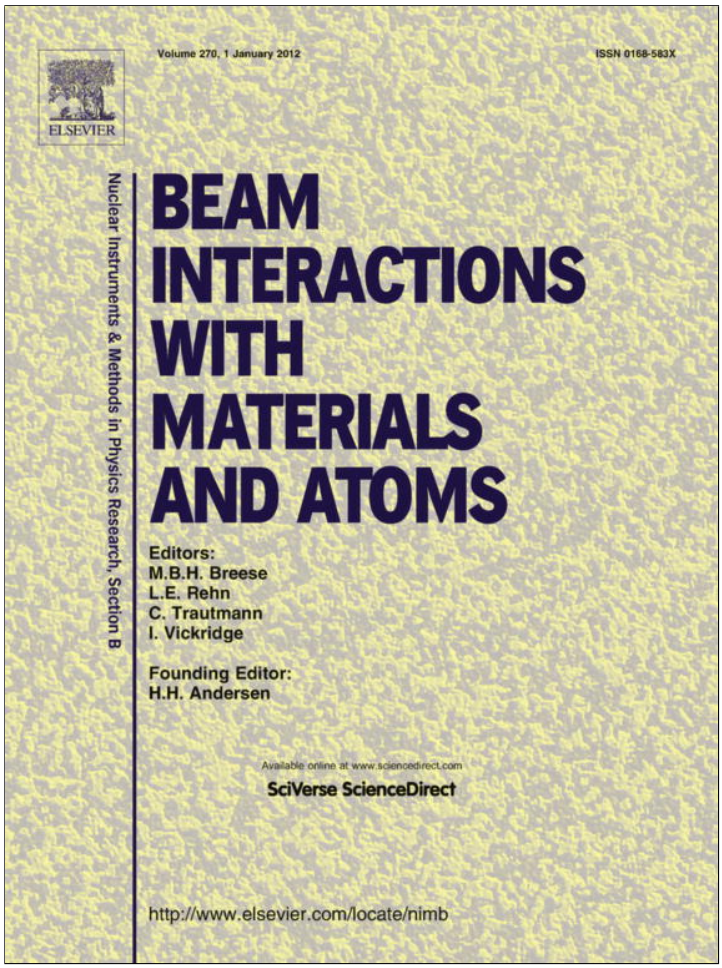

(This is a sample cover image for this issue. The actual cover is not yet available at this time.)

Nuclear Instruments and Methods in Physics Research B 296 (2013) 7–13

Contents lists available at SciVerse ScienceDirect

Nuclear Instruments and Methods in Physics Research B

journal homepage: www.elsevier.com/locate/nimb

Analysis of Roman glass from Albania by PIXE–PIGE method

Ž. Šmit [a,b,*], F. Tartari [c], F. Stamati [d], A. Vevecka Priftaj [e], J. Istenič [f]

[a] University of Ljubljana, Faculty of Mathematics and Physics, Jadranska 19, SI-1000 Ljubljana, Slovenia
[b] Jožef Stefan Institute, Jamova 39, P.O. Box 3000, SI-1001 Ljubljana, Slovenia
[c] Institute of Archaeology, Tirana, Albania
[d] Institute of Folk Culture, Laboratories of Conservation, Kont Urani 3, Tirana, Albania
[e] Polytechnic University of Tirana, Sheshi Nene Tereza 4, Tirana, Albania
[f] National Museum of Slovenia, Prešernova 20, SI-1000 Ljubljana, Slovenia

ARTICLE INFO

Article history:
Received 5 October 2012
Received in revised form 4 December 2012
Available online 20 December 2012

Keywords:
Roman glass
PIXE
PIGE
Albania

ABSTRACT

A series of 31 Roman glasses dated to the 1st–4th c. AD from the present Albania was analyzed by the combined PIXE–PIGE method. The analysis shows typical natron-based glass of the Roman period, though statistical treatment using principal component analysis and bivariate plots reveals four distinct groups, which are qualified by increased levels of potassium, magnesium and titanium–manganese–iron oxides, respectively. MgO content may exceed 2% and reach the level commonly accepted for halophytic plant-ash glass. The groups are formed on account of mineral impurities in the sand, which gives support to the thesis of multiple production centers of raw glass in the imperial age.

1. Introduction

The territory of the present Albania had intense contacts with the Romans since the late 3rd century BC onwards. The Illyrian city of Lissus and Greek colonies of Apollonia and Dyrrachium were used as temporary Roman bases in Illyrian and Macedonian wars. The Roman province of Illyricum was established in 135 BC, though a Roman colony is documented in Dyrrachium since 30 BC. However, it was Augustan period that brought major improvements in glass production techniques including blown glass, which launched a booming glass industry for the following two centuries. In Albania, glass finds are recorded in the centers exhibiting elements of Roman civilization: Butrint, Apollonia, Dyrrachium, Bylis and several others, which are also characterized by commercial relation with Italy, as well as locations in the East (Greece, Asia Minor) and North Africa. Typologically, the glass types include medical and cosmetic glass (medicine bottles, vials, balsamaria, unguentaria), wrapping, laboratory and artistic glass (laboratory funnels, tubes, pipes, sprained neck vessels), and various types of ware for domestic use [1]. There is decline of glass finds from the 3rd and 4th centuries. The glass involved in the analysis originates from excavations in different locations in Albania, some of them discovered during the construction works of modern highways. An example is a concretized sand slab with numerous glass fragments, evidently part of a glass furnace. Excavations in the building complex in ancient Asparagium (modern Rogozhina) produced numerous fragments of vessels for daily use, together with fragments of window panes. The site also contained fragments of unfinished glass products together with the remains of the glass furnace.

The glass samples involved in the analysis are dated to the 1st–4th century AD according to their archeological context with a precision of a century. In our work we determined the major composition and specific minor elements and compared them to the composition of Roman glass from the other parts of Europe and Mediterranean; according to our knowledge no analytical work on the Roman glass from Albania has been done before. It is particularly interesting to look for individual properties of the glass, as production of raw glass in Roman times is still disputable. While a large-scale production of raw glass was practiced in Palestine and Egypt during Late Antiquity [2,3], local production centers may also be active during the imperial age [4–9]. It is interesting to mention that the Albanian coast also contains sand rich in silica, which could be a potential raw material for glass production.

2. Experimental

The analysis involved 32 glasses, acquired as fragments or sampled from larger fragment pieces; from the sand slab, three shreds were peeled off for analysis. Before analysis the samples were washed with alcohol. Freshly cleaved surfaces, resulting due to

* Corresponding author at: University of Ljubljana, Faculty of Mathematics and Physics, Jadranska 19, SI-1000 Ljubljana, Slovenia. Tel.: +386 1 4766589; fax: +386 1 2517281.
E-mail addresses: ziga.smit@fmf.uni-lj.si, ziga.smit@ijs.si (Ž. Šmit).

0168-583X/$ - see front matter © 2012 Elsevier B.V. All rights reserved.
http://dx.doi.org/10.1016/j.nimb.2012.12.007

sampling or in a few cases, due to excavation incidents were exposed to the beam if available with an area of a few mm^2 or more.

The analysis was made at the Jožef Stefan Institute in Ljubljana, using proton beam in air. The nominal proton energy was 3 MeV; after passing an Al window of 8 μm used for PIXE measurements, and a 1 cm air–gap, the energy at the target was about 2.7 MeV. The X-ray detector was positioned at 45° with respect to the target normal. The distance between target and detector was 5.7 cm, and the experimental geometry was kept fixed by nylon spacers. The intermediate air gap acted as an efficient absorber of silicon X-rays with a suppression factor of about 160. Precise values of the air–gaps were determined from the measurements of several elemental and simple chemical compound targets. The argon line, induced by protons in the gap between exit window and target, was used to determine the impact proton number [10]. For the detection of elements heavier than approximately iron, the measurement was repeated in the same spot using an additional absorber of 0.1 mm aluminum and increasing the proton current from a few tenths of nA to about 3 nA. The measuring time in both cases was 400–600 s. Since the Ar line was not seen in these spectra, the two types of spectra were combined into one using the iron Kα line for normalization.

The concentrations of elements lighter than silicon, whose X-rays were completely absorbed in the air, were determined according to the intensities of proton-induced gamma rays (PIGE). For this measurement the exit nozzle made of brass with an exit foil of 2 μm Ta was used, in order to reduce the production of background radiation to sub 300 keV energies. The impact energy at the target surface, after passing a 1.1 mm air gap, was about 2.76 MeV. The beam profile was approximately Gaussian, with 0.8 mm full-width at half maximum. The beam intensities were 2–4 nA and the irradiation time was about 2000 s. For measuring of the incident proton number, the proton current was collected from a thin wire mesh intersecting the beam in vacuum [11]. The transmission of the mesh was about 58%, and the collected charge for particular measurement was 5 μC. The induced gamma spectra were detected by a 40% intrinsic germanium detector. The observed gamma lines, produced by inelastic proton scattering, were 440 keV for Na, 585 keV for Mg, and 844 and 1014 keV for Al. Silicon lines of 1273 and 1779 keV, which are intensely produced at energies above 3.1 MeV [12], were observed with marginal counting statistics at our experiment [13]. The magnesium line of 585 keV interfered with 583 keV line from the natural background. The count rate of this line was measured and a correction applied. However, due to high Compton background of sodium 1634, 1636 keV lines and of the 583 keV contribution, the detection limit for Mg was about 0.2%. The concentrations of Na, Mg and Al were determined by the surface approximation [14] according to the NIST 620 glass standard. The procedure is matrix dependent, as the unknown concentrations depend on proton stopping in the target. Stopping powers and X-ray attenuation coefficients are also required for the evaluation of concentrations from the X-ray data. The unknown concentrations were then evaluated iteratively, calculating the matrix effects for X-rays and gamma rays simultaneously in each iteration step [13]. All elements were assumed to be in oxide form and the sum of all oxides was set to unity. As a measure of precision of the method, the sum of the metal oxides according to the intensity of the argon line was also determined. Departure of this value from unity within ±20% were regarded as acceptable and resulted in concentration uncertainties about 5% for major components and 10–15% for trace elements at the detection limits. As a further test of the procedure, the standards NIST 620 and 621 were measured periodically and analyzed as unknown samples.

3. Results

The elemental concentrations of 31 glass specimens are given in Table 1 in mass%. Sample number 20, initially resembling black

Table 1
Composition of the investigated glass-concentrations of oxides in mass%. Single zeros denote elements below the detection limits. Colors: LG–light green, BG–blue green, OG–olive green. For the color of sample 6 see text.

Glass	Age(AD)	Color	Na_2O	MgO	Al_2O_3	SiO_2	SO_3	Cl	K_2O	CaO	TiO_2	MnO	Fe_2O_3	NiO	CuO	ZnO	Br	Rb_2O	SrO	ZrO_2	Sb_2O_3	PbO
1	1–2	LG	14.0	0.59	3.61	66.5	0.57	1.17	0.60	10.3	0.088	1.90	0.47	0.0010	0.0022	0.0014	0.0007	0	0.062	0.0040	0	0.001
2	1–2	BG	16.2	0.57	2.74	68.7	0.47	0.96	1.60	7.96	0.060	0.30	0.45	0.0012	0.0164	0.0022	0.0006	0	0.050	0.0050	0.033	0.018
3	1–2	BG	16.0	0.25	2.78	68.9	0.58	1.13	0.70	8.65	0.064	0.51	0.34	0.0019	0.0060	0.0020	0.0006	0	0.053	0.0049	0	0.002
4	1–2	BG	15.2	0.78	3.34	69.1	0.44	1.01	1.41	7.68	0.065	0.34	0.48	0.0012	0.0031	0.0029	0.0007	0	0.055	0.0055	0	0.001
5	1–2	BG	16.2	0.89	2.14	67.6	0.52	1.19	0.71	9.84	0.064	0.50	0.35	0.0019	0.0129	0.0019	0.0005	0	0.055	0.0049	0.028	0.006
6	1–2		8.6	0.58	6.22	77.7	0.66	0.32	1.23	3.57	0.069	0.57	0.46	0.0017	0.0018	0.0013	0.0007	0	0.037	0.0074	0	0.001
7	1–2	BG	15.8	0.61	2.38	68.2	0.49	1.04	1.99	8.58	0.063	0.30	0.44	0.0016	0.024	0.0030	0.0009	0	0.050	0.0056	0.042	0.020
8	2	LG	16.7	0.27	1.97	70.8	0.55	0.69	1.54	6.32	0.074	0.27	0.40	0.0015	0.0040	0.0030	0.0008	0	0.047	0.0060	0.26	0.017
9	3–4	LG	16.0	0.54	2.42	67.2	0.51	1.27	1.58	8.76	0.065	1.20	0.33	0.0015	0.0040	0.0016	0.0007	0.0011	0.061	0.0056	0	0.001
10	3–4	OG	17.5	1.03	2.53	65.0	0.57	1.10	0.55	7.44	0.455	1.95	1.70	0.0021	0.0082	0.0032	0.0013	0	0.062	0.0292	0	0.007
11	3–4	OG	17.5	0.95	2.40	65.7	0.51	1.00	0.56	6.74	0.487	2.00	1.89	0.0032	0.0078	0.0033	0.0015	0	0.066	0.0365	0	0.005
12	3–4	OG	17.0	1.10	2.63	66.3	0.50	1.00	0.63	7.81	0.284	1.33	1.31	0.0023	0.0074	0.0034	0.0008	0.0008	0.069	0.0220	0	0.008
13	3–4	LG	16.3	0.51	2.46	66.1	0.62	1.46	0.76	10.1	0.074	1.16	0.28	0.0009	0.0019	0.0010	0.0005	0.0009	0.047	0.0047	0	0.001
14	1–2	BG	16.7	0.58	2.51	68.0	0.48	1.05	0.79	8.86	0.077	0.33	0.45	0.0014	0.025	0.0021	0.0004	0.0018	0.051	0.0048	0.040	0.027
15	2–3	BG	19.1	2.11	2.00	64.2	0.62	1.13	1.39	7.58	0.197	0.26	1.42	0.0015	0.0056	0.0040	0.0006	0.0006	0.050	0.0146	0.029	0.009
16	1–2	BG	16.5	0.63	2.40	68.2	0.52	1.11	0.73	8.93	0.069	0.35	0.39	0.0015	0.022	0.0020	0.0005	0.0008	0.050	0.0047	0.034	0.014
17	2–3	BG	18.7	1.89	1.87	65.7	0.61	1.05	1.22	6.88	0.174	0.28	1.47	0.0016	0.0053	0.0045	0.0005	0.0009	0.062	0.0193	0.032	0.012
18	2–3	BG	19.0	2.49	2.02	64.4	0.64	1.03	1.29	7.09	0.179	0.30	1.38	0.0015	0.0062	0.0048	0.0006	0	0.054	0.0135	0.048	0.014
19	3–4	BG	17.0	0.67	2.63	67.4	0.55	1.09	0.78	8.96	0.074	0.33	0.46	0.0014	0.027	0.0023	0.0005	0.0016	0.051	0.0046	0.047	0.027
21	3–4	LG	14.6	0.50	2.27	71.5	0.57	1.20	0.66	8.40	0.058	0.02	0.31	0.0011	0.0009	0.0014	0.0005	0	0.048	0	0	0.001
22	3–4	BG	14.6	0.39	2.65	70.6	0.51	1.18	0.82	8.40	0.066	0.51	0.31	0.0016	0.0008	0.0018	0.0004	0.0010	0.054	0	0	0.001
23	3–4	BG	19.6	2.24	2.00	64.8	0.63	1.06	1.21	6.58	0.185	0.23	1.31	0.0013	0.0058	0.0041	0.0008	0.0007	0.052	0.0139	0	0.009
24	3–4	LG	15.2	0.49	2.25	69.7	0.64	1.21	0.63	8.96	0.073	0.24	0.40	0.0015	0.0014	0.0017	0.0007	0.0007	0.046	0.0048	0	0.001
25	3–4	BG	14.4	0.78	2.12	71.0	0.49	1.07	1.39	8.17	0.052	0.05	0.40	0.0020	0.0029	0.0023	0.0003	0.0010	0.055	0.0061	0	0.002
26	3–4	LG	15.4	0.37	2.06	70.8	0.52	1.18	0.74	8.61	0.058	0.03	0.25	0.0010	0.0012	0.0012	0.0003	0.0011	0.046	0.0037	0	0.001
27	3–4	LG	15.2	0.64	2.44	68.0	0.57	1.17	1.98	8.44	0.062	1.10	0.31	0.0015	0.0052	0.0015	0.0006	0.0009	0.059	0.0056	0	0.001
28	3–4	BG	14.3	0.64	2.89	71.5	0.44	0.85	1.33	7.49	0.071	0.05	0.45	0.0020	0.0016	0.0017	0.0002	0.0014	0.044	0.0045	0	0.001
29		LG	12.7	0.46	4.99	69.1	0.48	0.17	1.40	9.77	0.179	0.05	0.56	0.0040	0.0027	0.0034	0	0.0048	0.013	0.0117	0	0.006
30		LG	14.2	0.76	2.53	72.3	0.34	0.70	0.75	7.16	0.071	0.57	0.43	0.0016	0.0064	0.0026	0.0004	0.0007	0.053	0.0042	0.13	0.031
30–1		BG	15.9	0.60	2.78	68.9	0.63	1.07	0.66	7.92	0.088	0.68	0.45	0.0019	0.0066	0.0026	0.0005	0.0009	0.052	0.0050	0.15	0.034
30–2		BG	15.2	0.55	2.17	72.1	0.58	0.81	0.60	6.56	0.077	0.61	0.43	0.0017	0.0063	0.0051	0.0004	0.0008	0.053	0.0058	0.15	0.032

opaque glass was omitted from the table, as it was recognized as a charred bone fragment. The elemental concentrations not detected are shown by single zeros. The detection limits for the elements that were not detected in all samples are 300 μg/g for Br and Rb, and about 1000 μg/g for Sb. Most of the analyzed samples were of blue–green or light green color in different shades, therefore no elements characteristic for intentional pigmentation or opacifying were observed. The detection limit for Co was about 100 μg/g and for Sn about 1000 μg/g.

4. Discussion

All analyzed samples represent sodium-type glass with sodium concentrations between 14 and 19.6% Na_2O; the only exception is sample six which contains 8.6% Na_2O. This low value, which implies an atypically high SiO_2 content of 77.7%, may be result of corrosion. The sample surface is rough and of milky appearance, though transparent glass can be noticed in a tiny area where the fragment was broken. In our further analysis, this sample will be interpreted with caution.

The glasses in Table 1 do not appear homogeneous; therefore we tried to distribute them in characteristic groups using statistical techniques. Hierarchical clustering are usually applied for this purpose [6,7,15–18], however, we preferred to use the principal component analysis, as in addition to characteristic groups it also reveals significant discriminating elements and relations among them [19]. Both methods are based on the Euclidean distance of concentration differences and normally apply data standardization, i.e. transformation of data to zero mean and unity standard deviation. Our PCA code is based on the review of Clayton [20] and includes a procedure of non-linear mapping of Sammon [21]. Further, instead of transforming the data to zero mean and unity standard deviation we used the logarithmic transformation $c_i' = \ln(1 + c_i)$ of Duewer [20], which similarly suppress the influence of high concentrations.

The classification into groups was done according to the concentrations of eight elemental oxides (of Na, Mg, Al, Si, K, Ca, Ti and Fe), as suggested by Picon, Vichy and Thirion–Merle [16,17]. Different elements are used in other works, for example the same authors omitted Na, as it is not pertinent to the sand component of the glass [22], and Mirti [15] omitted Si and Fe and used the trace elements Sr and Ba instead. PCA graph of the Roman glasses from Albania clearly shows three groups (Fig. 1a). The largest group seems to be divided into two subgroups which we denote by 1a and 1b; this division will appear clear in Fig. 1b. The other two smaller groups contain four and three members, respectively: group 2 contains all three glasses assigned to the 2nd–3rd centuries and one glass of the 3rd–4th centuries. The third group is composed of three 3rd–4th c. glasses of olive-green color; these are fragments of window glass from Asparagium. It is characteristic for this group that the content of TiO_2 is higher than 0.28% and those of Fe_2O_3 and MnO higher than 1.3% (Table 1), which is in the range of HIMT glass [15]. This type of glass appeared in the 4th c. AD and was made of sand with a much higher level of impurities [3,9,15,23]. Sample 6 with its low Na_2O content understandably appears as outsider in Fig. 1a. The stern of eigenvectors in Fig. 1a shows that the selected elements are of nearly equal importance for glass characterization, except potassium, whose eigenvector is about five times shorter than that of aluminum, which is its nearest.

The groups identified by PCA are clearly reproduced in the bivariate plot of K_2O against Na_2O (Fig. 1b), which is usually used for distinction of natron and plant-ash based flux [24]. Group 1 now decomposes into two subgroups, 1a and 1b. The subgroup 1a and group 3 exhibit MgO values below 1.1% and K_2O values below 0.8%, which agrees with the limits of 1.47% and 0.63% determined for the two elements in natron-type glass [25]. It is also evident that higher MgO values (between 0.95 and 1.1%) are contained in group 3, while the concentrations below 0.89% are observed in the 1st–2nd c. and 3rd–4th c. glass. The subgroup 1b with a similar age structure shows similarly low MgO values (below 0.78%), but its K_2O concentrations are higher, approaching 2% in two samples, which exceeds the limits accepted for natron-type glass. Subgroup 1b also contains the outlier, sample 6.

MgO levels between 1.89 and 2.49% are observed for group 2, which are the values in the range of plant-ash glass, whose occurrence is recorded in Europe after 800 AD. However, improper dating of all four samples in group 2 is not probable, nor they could be mistaken by some other, later type of glass because the glasses were found in a well defined chronological context. On the other hand, several arguments can be found that point group 2 as a natron-type glass produced of sand with different impurities. This supposition is in accordance with the view that primary glass was produced with the Egyptian natron, but using sand of different origins. Beside the primary glassworks in Palestine and Egypt, which experienced massive production of glass at least in Late

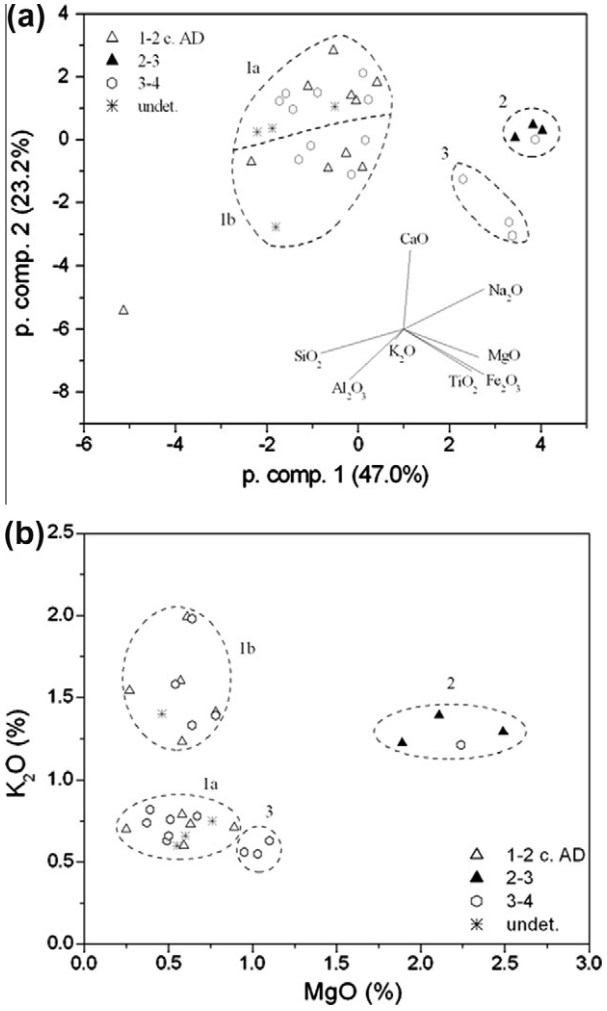

Fig. 1. (a) Distribution of glasses according to the principal component analysis (PCA) using the oxides of Na, Mg, Al, Si, K, Ca, Ti and Fe. For the sake of clarity, the lengths of eigenvectors were multiplied by four. Sample 8 (2nd c.) was plotted among the 1st-2nd c. glasses. Subgroup 1a involves samples 1, 3, 5, 13, 14, 16, 19, 21, 22, 24, 26, 30 (0–2) and subgroup 1b samples 2, 4, 7, 8, 9, 25, 27, 28, 29. Group 2 is composed of samples 15, 17, 18, 23 and group 3 of 10, 11, 12 (Table 1). The outsider is sample 6. (b) Bivariate plot of K_2O against MgO revealing the same groups, except sample 6 joining the subgroup 1b.

Antiquity [2], Roman imperial age glass could also be produced in Italy, south France and Spain, as suggested by the writings of Strabo and Pliny [26,27,5]. Crucibles exposed to high temperature suggest that raw glass might have been produced in Coppergate, England [28], while the sand of the Rur River represented the siliceous component of glass found in Hambach, Germany [29]. One piece of glass with the composition of 2.62% MgO and 1.85% K_2O was found among the colored glass of the Iulia Felix shipwreck dated to the first half of 3rd c. AD [7] and three glasses exhibiting MgO concentrations between 2.09 and 3.08% and K_2O values between 1.02 and 1.94% were discovered among the Roman imperial glass of Canton Ticino in Switzerland [18].

Roman mosaic glass exhibits even more diverse composition [30]. Elevated levels of magnesium, potassium and phosphorous demonstrate that particular glasses were made of plant ash. The predominant colors were red, orange and green, pigmented by copper at about 1% level. Several glasses showed higher levels of magnesium, but not potassium and phosphorous; they were likely made of natron, with magnesium originating from dolomite component of the sand, particular type of the flux, or dolomite background of antimony–lead ores used for discoloration [31].

Among the post-Roman glass, two specimens showing MgO concentrations of 1.84 and 1.91% and K_2O concentrations of 1.87 and 2.04% were encountered between the early Byzantine glass of the 6th and 7th centuries, excavated in Caričin grad (Serbia), which lead the authors to identify them as an early example of plant-ash glass [32].

Occurrence of plant-ash glass among the imperial age Roman glass is not impossible, as the tradition of plant-ash glassmaking was continuously practiced in Mesopotamia. As the glass fragments carried on Iulia Felix were intended for recycling, diffusion of some pieces of plant-ash glass among the glass batch is not improbable [32]; such glass may also be an Egyptian antiquity predating the natron period that began around 4th c. BC [18], or even earlier as testified by the analysis of Theban glass beads of archaic period [33]. However, Silvestri argued that all glass of Iulia Felix is natron-type, notably on account of SO_3 and Cl contents typical of natron composition [7]; natron composition is variable, but contains 22.4–75.0% sodium carbonate, 5.0–32.4% sodium bicarbonate, 2.2–26.8% sodium chloride and 2.3–29.9% sodium sulfate [34]. Inspection of Table 1 shows that group 2 (samples 15, 17, 18 and 23) show both high SO_3 and Cl values, characteristic for natron. Further, in PCA plot of Fig. 1a, magnesium appears correlated with iron and titanium, which are normally related to the mineral impurities in sand. Low K_2O values below 1.5% characterize this glass as magnesium type according to [30]. Made by natron, magnesium was introduced into the glass batch as a mineral impurity from the sand. Beside dolomite, magnesium is also constituent of olivine and magnesium-rich pyroxenes. In both minerals it is accompanied by iron; Fe_2O_3 concentrations between 1.31–1.47% in group 2 are only slightly lower than those of HIMT glass (group 3).

Group 1b in Fig. 1b is characterized by high K_2O, but low MgO values. Glass with low MgO values but K_2O concentrations above 2% were also detected among the post-Roman natron-type glass in Slovenia [35,13]. However, the occurrence of such glass is not common, as only low MgO and K_2O glasses were found among the analyzed glass from Dalmatia [36]. In the PCA plot of Fig. 1a, potassium and aluminum eigenvectors appear parallel, so the increased concentration of potassium may be due to potassium containing minerals, like alkali feldspars. These can be present in primary raw materials as impurities, but they can also be constituents of the furnace walls either in primary or secondary workshops.

Fig. 1 suggests that different sands were used for production of the investigated glass from Albania. This is further corroborated in the Al_2O_3–CaO bivariate plot (Fig. 2) and in the level of the elements present as impurities (Fig. 3). Fig. 2 shows the measured values together with the areas of Roman imperial age glass from south France (groups 3^- and 4 of Foy et al. [22]) and from the shipwreck of Iulia Felix (groups 1, 2 of colored glass according to Silvestri) [7]. For the group 3^- of Foy, the values for the imperial age glass were determined subtracting the contributions of the subgroups 3.1–3.3, which comprise Late Roman glass since the end of the 4th century onwards [22]. Of the late Roman glass we show the subgroup 3.1 of Foy [22], dated from the end of the 4th c. to the beginning of the 5th century; this group is related to the Levantine I group of Freestone, which spans the time interval of 5th–7th century [3]. The regions of these (sub)groups are shown as ellipses with the ax lengths of four standard deviations, except for the groups of Levantine I and HIMT, which are drawn by squares in the way as introduced by Zucchiatti [24]. Fig 2 reveals that the majority of samples agrees best with the group 3^- of Foy (group 3 reduced for the subgroups 3.1–3.3 of Late Roman glass), which was produced using sand of the region around Belus River in Palestine, roughly extending between Sidon and Tel Aviv [16]. The two groups of Iulia Felix agree reasonable well with this group, dividing it into two parts. Group 4 of Foy, identified among the glass of the 3rd century shipwreck Ouest Embiez, is only modestly present among the investigated glass; it is only glass eight, dated to the 2nd century, which can be assigned to this group. Group 4 of Foy is yet of unknown origin and involves glasses of the 2nd and 3rd centuries; its main characteristic is discoloration by antimony [22]. Group 3.1 of Foy covers the high Al_2O_3–CaO part of the distribution of Fig. 2; it is embedded in the Levantine I group [3]. As expected, only a few of the measured glasses coincide with this group, though two were provisionally dated to an earlier period. Only a few glasses appear outsiders in Fig. 2, the most prominent being samples 6 and 29.

The samples of group 2 (as defined in Fig. 1), characterized by low Al_2O_3 values of about 2%, appear slightly separated from the established groups in Fig. 2, which may suggest a different sand source. Properties of the sand are studied in bivariate plots of minor elements in Fig. 3. Both groups 2 and 3 exhibit a much higher Fe_2O_3 content between 1.3 and 1.9% (Fig. 3a). Titanium in the two groups is correlated to iron (Fig. 3b), but the two correlation lines differ. Lower TiO_2 values in group 2 may also suggest recy-

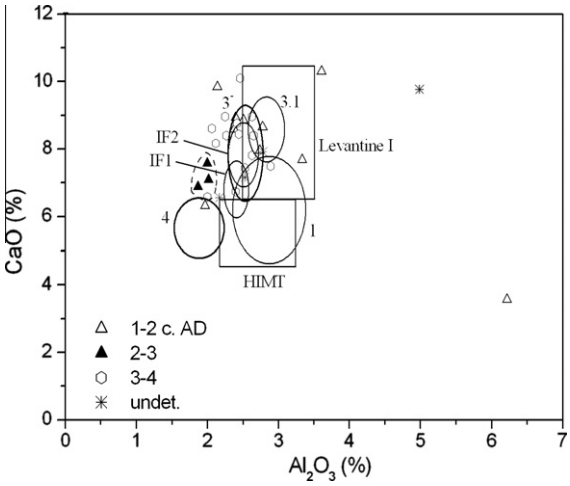

Fig. 2. Bivariate plot of CaO against Al_2O_3 with the areas of Roman imperial glass of Foy (groups 3^- and 4) [22], Iulia Felix (colored glass groups 1 and 2) [7] and Late Roman glass of 4th-early 5th c. AD: groups 1 and 3.1 of Foy [22], HIMT and Levantine I glass [3,24]. The ellipses have diameters of four standard deviations. Of the groups found in Fig. 1, only the group 2 is shown. The three glasses of group 3 are located in the lower part of Foy's group 3^-. The outliers are samples 29 and 6.

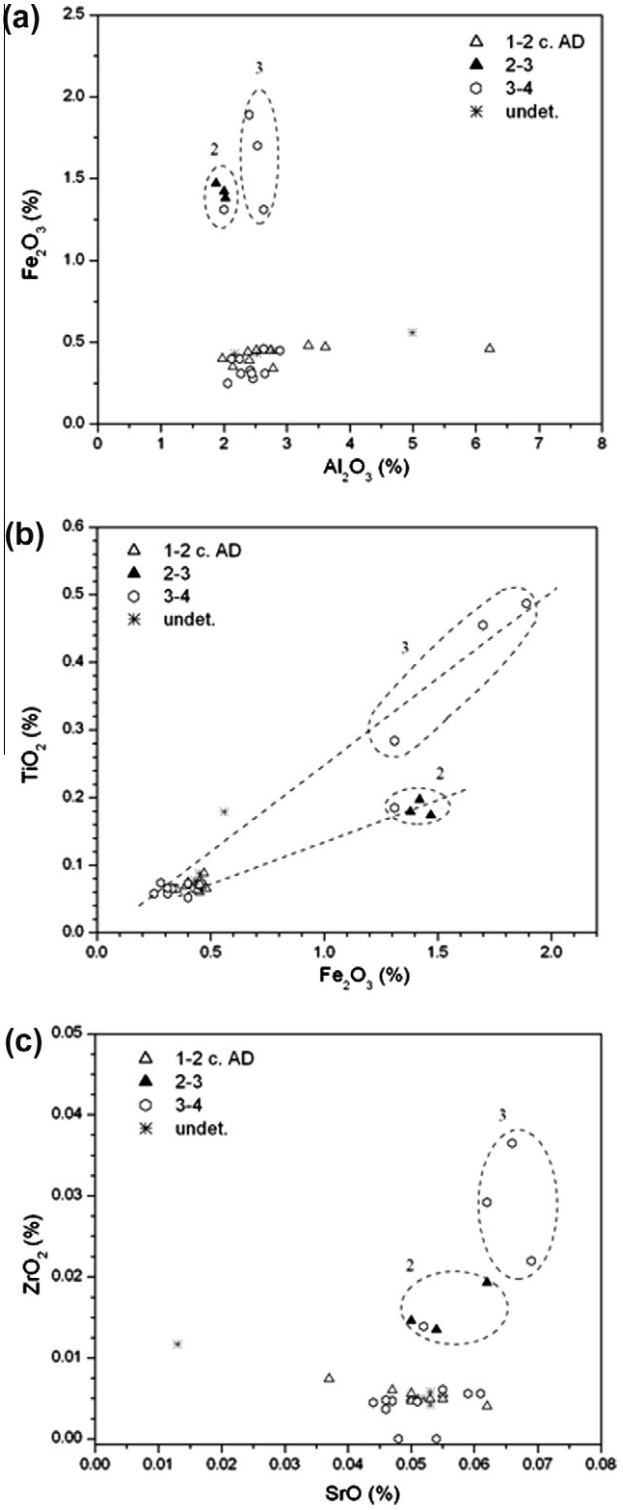

Fig. 3. Impurities in the sand component of the glass. Bivariate plots of (a) Al_2O_3–Fe_2O_3, (b) Fe_2O_3–TiO_2, and (c) SrO–ZrO_2.

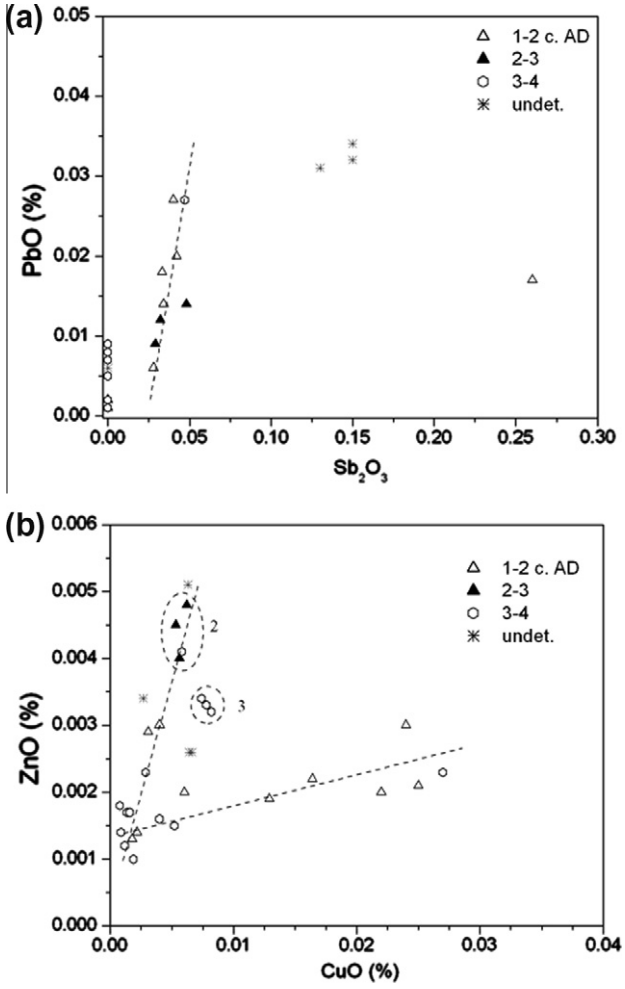

Fig. 4. Trace elements: PbO against Sb_2O_3 (a) and ZnO against CuO (b). The lines are drawn by eye.

cling with a certain quantity of HIMT glass, but this glass was not available in the 2nd–3rd centuries. The groups 2 and 3 remain compact also in the SrO – ZrO_2 plot (Fig. 3c), and are characterized by a high zirconium content. The highest strontium and zirconium values are manifested for group 3. Composition of this group is closest to HIMT glass; however, its CaO content is higher than typical for HIMT glass (Fig. 2) and it matches with the lower values of group 3^- of Foy. This indicates that our group 3 is very likely composed of HIMT glass that was recycled with the group 3^- (Foy) glass. On the other hand, group 2 with its specific contents of MgO (Fig. 1), Al_2O_3–CaO (Fig. 2) and impurity pattern (Fig. 3) may indicate an individual sand source.

SrO values in Fig. 3a are above 350 μg/g, which is consistent with the use of coastal sand in making of the raw glass [3]. The only significant exception is glass 29, which appears as an outsider also in graphs of Fig. 2 and 3. Its low SrO content of 130 μg/g suggests it was made of limestone bearing sand [3].

Roman glass was discolored by addition of antimony or manganese oxides. Antimony was twice more effective than manganese and was usually applied for discoloration of high-quality materials [4]. The use of antimony was introduced in the late 1st c. BC [9], but declined after the 3rd c. AD. Discoloration with antimony is characteristic of Foy's group 4 [22]. Intentional discoloration was achieved by antimony levels above 0.2% [25] and by manganese levels above 0.5% [4], lower levels being result of mixing different types of glass in the recycling process. According to Silvestri [7], all glasses below a certain level of Sb_2O_3 (set to 0.82 ± 0.11%, from the values observed in the colored glass of Iulia Felix shipwreck) were subject to recycling. Among the glasses in Table 1, only the sample 8 showing 0.26% Sb_2O_3, appears to be discolored with antimony. However, its K_2O and MgO levels are a bit high for Foy's group 4, though still within ± 2σ range (Fig. 2). It is not impossible that the sample 8 is of recycled glass that retained a significant contribution of group 4 component. The three undetermined glasses

originating from highway excavation (30, 30–1, 30–2 in Table 1) contain about 0.15% Sb_2O_3, while the remaining glasses exhibit less than 0.05% Sb_2O_3, which undoubtedly reflects recycling. Antimony might have been added into the glass batch in the form of stibnite Sb_2S_3 [6], which may be associated to sulfides of several other elements, such as Cu, Pb, Zn, Cd and As [34]. The respective ratio of Sb to certain elements is characteristic of the antimony source and is preserved at the dilution process. Fig. 4a shows a bivariate plot of PbO against Sb_2O_3. Several glasses, dated to the 1st–3rd centuries (and one, dated to the 3rd–4th centuries) are collected along a line with a slope of 1.2. This value exceeds the highest Pb/Sb ratios in Huisman [37] by an order of magnitude, which may point to a radically different antimony source.

The recycling history is further reflected in the level of impurity elements, which serve for pigmentation [3]. A specific case is blue color which was achieved by addition of copper and cobalt oxides [15]. Fig. 4b shows the concentration of ZnO with respect to CuO. Two correlation lines are observed. The lover one, with a slope of 0.05, is mainly related to the 1st-2nd century glasses. The source of copper may include brass. The second correlation line with a slope of 0.7 connects data of different periods, including those of group 2. Glasses of group 3 stay apart of the two lines but remain grouped. The impurity pattern, which reproduces groups 2 and 3, suggests that each group can also be related to a specific secondary workshop.

5. Conclusions

The investigated Roman glass from the territory of the present Albania is typical natron-type glass, but showing individual properties due to its sand component. An important finding involves two groups of glass showing higher levels of potassium and magnesium oxides. While the potassium group is still close to the limits accepted for using natron as flux, the concentrations of magnesium oxide exceed 2% and therefore contact the region denoting flux made of halophytic plants. Examples of halophytic plant ash glass are encountered among the Roman mosaic glass. In addition, our survey of analytical results found some more examples of magnesium-rich Roman glass – one among the glasses of Iulia Felix and three from Canton Ticino, which suggests that the natron-type glass could acquire increased levels of K_2O or MgO from the sand component of the primary glass. The source of the two elements may be alkali feldspars, dolomite and magnesium-rich pyroxenes, respectively. The majority of the analyzed glass coincides with the Roman imperial glass component of Foy's group 3^- or the two groups of colored glass of Iulia Felix. Only one specimen, dated to the 2nd c. AD was discolored by antimony and can be associated with the group 4 of Foy. A small group of three samples exhibit increased levels of titanium, iron and manganese, though their CaO and Al_2O_3 concentrations do not qualify them as HIMT glass, but they were very likely recycled using HIMT glass. The recycling process is further demonstrated in Cu and Zn concentrations, which suggests that the detected groups are also specific for their secondary workshops. Individual properties of particular groups thus point to distinct sand sources of the raw glass and therefore support the thesis of dispersed production of primary glass during the imperial age.

References

[1] F. Tartari, La nécropole du Ier-IVe s c. de notre ère à Durrachium, Pal Engjëlli, Durrës, 2004. pp. 63–69.

[2] I.C. Freestone, Y. Gorin-Rosen, M.J. Hughes, Primary glass from Israel and the production of glass in Late Antiquity and the early Islamic period, in: M.-D. Nenna (Ed.), La route du verre. Ateliers primaries et secondaires du second millénaire av. J.-C. au Moyen Âge, Maison de l'Orient Méditerranéen-Jean Pouillox, Lyon, 2000, pp. 65–83.

[3] I.C. Freestone, The provenance of ancient glass through compositional analysis, Material Research Society Proceeding 852 (2005) OO8.1.1-13.

[4] C.M. Jackson, Making colourless glass in the Roman period, Archaeometry 47 (2005) 763–780.

[5] A. Silvestri, G. Molin, G. Salviulo, Sand for Roman glass production: an experimental and philological study on source of supply, Archaeometry 48 (2006) 415–432.

[6] A. Silvestri, G. Molin, G. Salviulo, The colourless glass of Iulia Felix, J. Arch. Sci. 35 (2008) 331–341.

[7] A. Silvestri, The colored glass of Iulia Felix, J. Arch. Sci 35 (2008) 1489–1501.

[8] K.A. Leslie, I.C. Freestone, D. Lowry, M. Thirlwall, The provenance and technology of near eastern glass: oxygen isotopes by laser fluorination as a complement to strontium, Archaeometry 48 (2006) 253–270.

[9] R. Arletti, G. Vezzalini, S. Benati, L. Mazzeo Saracino, A. Gamberini, Roman window glass, a comparison of findings from three different Italian sites, Archaeometry 52 (2010) 252–271.

[10] Ž. Šmit, M. Uršič, P. Pelicon, T. Trček-Pečak, B. Šeme, A. Smrekar, I. Langus, I. Nemec, K. Kavkler, Concentration profiles in paint layers studied by differential PIXE, Nucl. Instr. Meth. B 266 (2008) 2047–2059.

[11] D. Jezeršek, Ž. Šmit, P. Pelicon, External beamline setup for plated target investigation, Nucl. Instr. Meth. B 268 (2010) 2006–2009.

[12] A. Savidou, X. Aslanoglou, T. Paradellis, M. Pilakouta, Proton induced thick target γ-ray yields of light nuclei at the energy region Ep = 1.0–4.1 MeV, Nucl. Instr. Meth. B 152 (1999) 12–18.

[13] Ž. Šmit, T. Knific, D. Jezeršek, J. Istenič, Analysis of early medieval glass beads – Glass in the transition period, Nucl. Instr. Meth. B 278 (2012) 8–14.

[14] A. Climent-Font, A. Muñoz-Martin, M.D. Ynsa, A. Zucchiatti, Quantification of sodium in ancient Roman glasses with ion beam analysis, Nucl. Instr. Meth. B 266 (2008) 640–648.

[15] P. Mirti, A. Casoli, L. Appolonia, Scientific analysis of Roman glass from Augusta Praetoria, Archaeometry 35 (1993) 225–240.

[16] M. Picon, M. Vichy, D'Orient en Occident: l'origine du verre à l'époque romaine et Durant le haut Moyen Âge, in: D. Foy, M.-D. Nenna (Eds.), Échange et commerce du verre dans la monde antique. Actes du colloque de l'Association Française pour l'Archéologie du Verre, Aix-en-Provence et Marseille 2001, Éditions Monique Mergoil, Montagnac (2003), pp. 17-31.

[17] V. Thirion-Merle, M. Vichy, Annexe – Note sur la composition chimique des verres de l'épave des Embiez, Revue archéologique de Narbonnaise 40 (2007) 266–268.

[18] R. Arletti, G. Vezzalini, S. Biaggio-Simona, F. Maselli Scotti, Archaeometrical studies of Roman imperial age glass from Canton Ticino, Archaeometry 50 (2008) 606–626.

[19] M.J. Baxter, C.E. Buck, Data handling and statistical analysis, in: E. Ciliberto, G. Spoto (Eds.), Modern analytical methods in art and archaeology, J. Wiley and Sons, New York, 2000, pp. 681–746.

[20] Clayton, Some statistical techniques for provenacing artifact material: A user's view, in: W. Ambrose, P. Duerden (Eds.), Archaeometry: An Australian perspective, Australian National University Press, Canberra, (1982), pp. 90–99.

[21] J.W. Sammon, A nonlinear mapping for data structure analysis, IEEE Trans. Computers C 18 (1969) 401–409.

[22] D. Foy, M. Picon, M. Vichy, V. Thirion-Merle, Caractérisation des verres de la fin de l'Antiquité en Méditerranée occidentale: l'emergence de nouveaux courants commerciaux, in: D. Foy, M.-D. Nenna (Eds.), Échange et commerce du verre dans la monde antique. Actes du colloque de l'Association Française pour l'Archéologie du Verre, Aix-en-Provence et Marseille 2001, Éditions Monique Mergoil, Montagnac, 2003, pp. 41–85.

[23] A. Aerts, B. Velde, K. Janssens, W. Dijkman, Change in silica sources in Roman and post-Roman glass, Spectrochimica acta B 58 (2003) 659–667.

[24] A. Zucchiatti, L. Canonica, P. Prati, A. Cagnana, S. Roascio, A. Climent-Font, PIXE analysis of V-XVI century glasses from the archaeological site of San Martino di Ovaro (Italy), J. Cult. Herit. 8 (2007) 307–314.

[25] E.V. Sayre, R.W. Smith, Compositional categories of ancient glass, Science 133 (1961) 1824–1826.

[26] M.D. Nenna, M. Picon, M. Vichy, Ateliers primaries et secondaires en Égypte à l'époque Gréco-Romaine, in: M.-D Nenna (Ed.), La route du verre. Ateliers primaries et secondaires du second millénaire av. J.-C. au Moyen Âge, Maison de l'Orient Méditerranéen-Jean Pouillox, Lyon, 2000, pp. 97–112.

[27] S.D. Fontaine, D. Foy, L'épave Ouest-Embiez 1, Var, Le commerce maritime du verre brut et manufacturé en Méditerranée occidentale dans l'Antiquité, Revue archéologique de Narbonaise 40 (2007) 235–268.

[28] C.M. Jackson, L. Joyner, C.A. Booth, P.M. Day, E.C.W. Wager, V. Kilikoglou, Roman glass-making at Coppergate, York? Analytical evidence for the nature of production, Archaeometry 45 (2003) 435–456.

[29] K.H. Wedepohl, K. Simon, A. Kronz, Data on 61 chemical elements for the characterization of three major glass compositions in Late Antiquity and the Middle Ages, Archaeometry 53 (2011) 81–102.

[30] M.D. Nenna, B. Gratuze, Étude diachronique des compositions de verres employé dans les vases mosaïqués antiques: Résultats preliminaries, Annales du 17e Congrès AIHV (2006), University Press Antwerp, 2009.

[31] J. Henderson, Chemical and structural analysis of Roman enamels from Britain, in: E. Pernicka, G.A. Wagner (Eds.), Archaeometry '90, Birkhäuser Verlag, Bâle, 1991, pp. 285–294.

[32] J. Drauschke, S. Greiff, Chemical aspects of Byzantine glass from Caričin grad/Iustiniana Prima (Serbia), in: J. Drauschke, D. Keller (Eds.), Glass in Byzantium – production, usage, analyses, Verlag des Römisch-Germanischen Zentralmuseum, Mainz, 2010, pp. 25–46.

[33] D. Sokaras, A.G. Karydas, A. Oikonomou, N. Zacharias, K. Beltsios, V. Kantarelou, Combined elemental analysis of ancient glass beads by means of ion beam, portable XRF, and EPMA techniques, Anal. Bioanal. Chem. 395 (2009) 2199–2209.
[34] A.F.B. Aerts, K. Janssens, B. Velde, F.C.V. Adams, H. Wouters, Analysis of the composition of glass objects from Qumrân, Israel, and comparioson with other Roman glass from Western Europe, in: M.-D. Nenna (Ed.), La route du verre. Ateliers primaries et secondaires du second millénaire av. J.-C. au Moyen Âge, Maison de l'Orient Méditerranéen-Jean Pouillox, Lyon (2000), p. 113–121.
[35] Ž. Šmit, D. Jezeršek, T. Knific, J. Istenič, PIXE–PIGE analysis of Carolingian period glass from Slovenia, Nucl. Instr. Meth. B 267 (2009) 121–124.
[36] K. Tantrakarn, N. Kato, A. Hokura, I. Nakai, Y. Fujii, S. Gluščević, Archaeological analysis of Roman glass excavated in Zadar, Croatia, by newly developed portable XRF spectrometer for glass, X-ray Spectrom. 38 (2009) 121–127.
[37] D.J. Huisman, T. De Groot, S. Pols, B.J.H. Van Os, P. Degryse, Compositional variation in Roman colourless glass objects from the Bocholtz burial (The Netherlands), Archaeometry 51 (2009) 413–439.